MOL PHARM

MOLECULAR PHARMACOLOGY

Multiple Interactions between Transmembrane Helices Generate the Oligomeric α_{1b}-Adrenoceptor

Juan J. Carrillo,[1] Juan F. López-Giménez, and Graeme Milligan

Molecular Pharmacology Group, Division of Biochemistry and Molecular Biology, Institute of Biomedical and Life Sciences, University of Glasgow, Glasgow, Scotland, United Kingdom

ABSTRACT

Combinations of coimmunoprecipitation, single-cell fluorescence resonance energy transfer, and cell-surface time-resolved fluorescence resonance energy transfer demonstrated protein-protein interactions and quaternary structure for the α_{1b}-adrenoceptor. Self-association of transmembrane domain 1 and its interaction with the full-length receptor indicated a symmetrical interface provided by this domain. Lack of effect of mutation of the glycophorin-A dimerization-like region within this helix demonstrated that this did not provide the molecular mechanism. Multiple interactions were observed between the α_{1b}-adrenoceptor and fragments derived from its sequence. Fragments comprising transmembrane domains 3 and 4 and transmembrane domains 5 and 6, but not transmembrane domain 7, were also able to interact with the full-length receptor. Transmembrane domain 7 failed to interact significantly with any element of the receptor and was not transported to the cell surface after coexpression with the full-length receptor. Symmetrical interactions were also noted between fragments incorporating transmembrane domain 4, but this segment of the receptor failed to interact with transmembrane domains 1 and 2 or transmembrane domains 5 and 6. Time-resolved fluorescence resonance energy transfer studies were also consistent with contributions of transmembrane domains 1 and/or 2 and transmembrane domains 3 and/or 4 to protein-protein interactions within the quaternary structure of the α_{1b}-adrenoceptor, and with a contribution of transmembrane domains 5 and/or 6. These data are consistent with a complex oligomeric quaternary structure of the α_{1b}-adrenoceptor in which major, symmetrical interactions may define intradimeric contacts with other contributions, providing interdimer contacts to generate oligomeric complexes akin to those observed for murine rhodopsin. A model derived from this was developed.

A host of recent studies have demonstrated the capacity of G protein-coupled receptors (GPCRs) to form dimers or, potentially, higher-order oligomers (George et al., 2002; Milligan et al., 2003; Milligan, 2004a). Conclusions that GPCRs have quaternary structure have derived from a wide range of experimental approaches. These include the analysis of ligand binding studies (Armstrong and Strange, 2001), the coimmunoprecipitation of coexpressed but differentially epitope-tagged forms of GPCRs (Hebert et al., 1996; Jordan and Devi, 1999; Uberti et al., 2003), interactions between GPCR fragments detected in yeast two-hybrid studies (White

et al., 1998), the application of a variety of resonance energy transfer techniques (Angers et al., 2000; Overton and Blumer, 2000; Rocheville et al., 2000; Cheng and Miller, 2001; McVey et al., 2001; Ayoub et al., 2002; Mercier et al., 2002; Ramsay et al., 2002; Canals et al., 2003), the use of chemical cross-linkers (Guo et al., 2003; Klco et al., 2003), and various forms of functional reconstitution (Kobilka et al., 1988; Osuga et al., 1997; Lee et al., 2002; Baneres and Parello, 2003; Carrillo et al., 2003). Recent application of atomic force microscopy has indicated the in situ organization of murine rhodopsin to be complex in that both dimeric structures and arrays of dimers were observed (Liang et al., 2003).

At this time, understanding of the basis of GPCR dimerization/oligomerization is limited. Early evidence suggested key roles for both C- (Cvejic and Devi, 1997) and N- (AbdAlla et al., 1999) terminal elements in homodimeric interactions between rhodopsin-like family A GPCRs. Certain more re-

aspet

ABBREVIATIONS: GPCR, G protein-coupled receptor; APC, allophycocyanin; FRET, fluorescence resonance energy transfer; TM, transmembrane; TR-FRET, time-resolved fluorescence resonance energy transfer; PCR, polymerase chain reaction; PBS, phosphate-buffered saline; MOPS, 4-morpholinepropanesulfonic acid; PAGE, polyacrylamide gel electrophoresis; CFP, cyan fluorescent protein; eYFP, enhanced yellow fluorescent protein; HEK, human embryonic kidney; RIPA, radioimmunoprecipitation assay; N-TM, N-terminal extracellular region of the receptor linked to the sequence defining a specific transmembrane domain.

cent studies have also provided evidence for a role of the N-terminal region in dimerization of the yeast α factor receptor (Overton and Blumer, 2002) and that N-terminal glycosylation may also be important in particular GPCRs (Xu et al., 2003). However, the bulk of recent work in this area has concentrated on the contribution of the transmembrane (TM) helices. Evidence for a key role of TM6 in dimerization of the β_2-adrenoceptor (Hebert et al., 1996) is mirrored in the leukotriene B4 BLT1 receptor. A peptide corresponding to this region disrupted dimer formation, whereas peptides corresponding to the other TM helices were without effect (Baneres and Parello, 2003). Initial studies on the dopamine D2 receptor also used TM peptides and indicated a role for TM6 (Ng et al., 1996). A peptide corresponding to TM7 of this GPCR produced a similar effect but was without effect on apparent homodimers of the dopamine D1 and 5-hydroxytryptamine-1B receptors (Ng et al., 1996). In the case of the β_2-adrenoceptor, part of the rationale for selecting TM6 for study was the presence of a glycophorin-A dimerization interface-like sequence (GXXXGXXXL) in this region. A peptide corresponding to the sequence of TM6 reduced immunoreactivity corresponding to the β_2-adrenoceptor dimer, but when the above sequence within the peptide was converted to AXXXAXXXA, this was without effect (Hebert et al., 1996), implying a role for this motif in dimerization. Recent studies on the yeast α factor receptor have also indicated a key role for a similar GXXXG sequence (Overton et al., 2003). In this case, it is located in TM1, a region indicated previously to be a key element for dimerization as determined from interactions between coexpressed fragments of the GPCR (Overton and Blumer, 2002). These differences may simply reflect that multiple contact points are required to produce high-affinity interactions, particularly if GPCRs do form complex oligomeric arrays (Klco et al., 2003; Liang et al., 2003). For rho-

dopsin, intradimer contacts were indicated to involve TMs 4 and 5, whereas contacts to generate further structural organization were suggested to involve TMs 1 and 2 and, possibly, the third intracellular loop (Liang et al., 2003). Because most studies are unable to discriminate between dimers and higher-order oligomers, data suggesting contributions from different or multiple TM elements may not be incompatible.

The diversity of data available at this point suggests that no single set of interactions or common mechanism is able to explain the foundation of GPCR quaternary structure. In the current study, we have performed comprehensive mapping of interactions between distinct fragments of the α_{1b}-adrenoceptor and between these fragments and the full-length receptor using both coimmunoprecipitation and fluorescence resonance energy transfer (FRET)-based techniques. We record a number of both symmetrical and nonsymmetrical interactions that are consistent with complex oligomeric structure. These may explain why much of immunoprecipitated α_{1b}-adrenoceptor migrates with apparent high molecular mass and why older studies on GPCR structure, which used approaches such as target-size analysis, suggested they might exist within large macromolecular complexes.

Materials and Methods

All materials for tissue culture were supplied by Invitrogen (Carlsbad, CA). Reagents for time-resolved fluorescence resonance energy transfer (TR-FRET) were from PerkinElmer Life and Analytical Sciences (Boston, MA). All other chemicals were from Sigma Chemical (Poole, Dorset, UK) or Fisons (Loughborough, UK) and were of the highest grade available.

Construction of α_{1b}-Adrenoceptor Fragments and Mutants. Production and subcloning of fragments of the α_{1b}-adrenoceptor was carried out in three steps. In the first step, the N-terminal domain of the hamster α_{1b}-adrenoceptor was ampli-
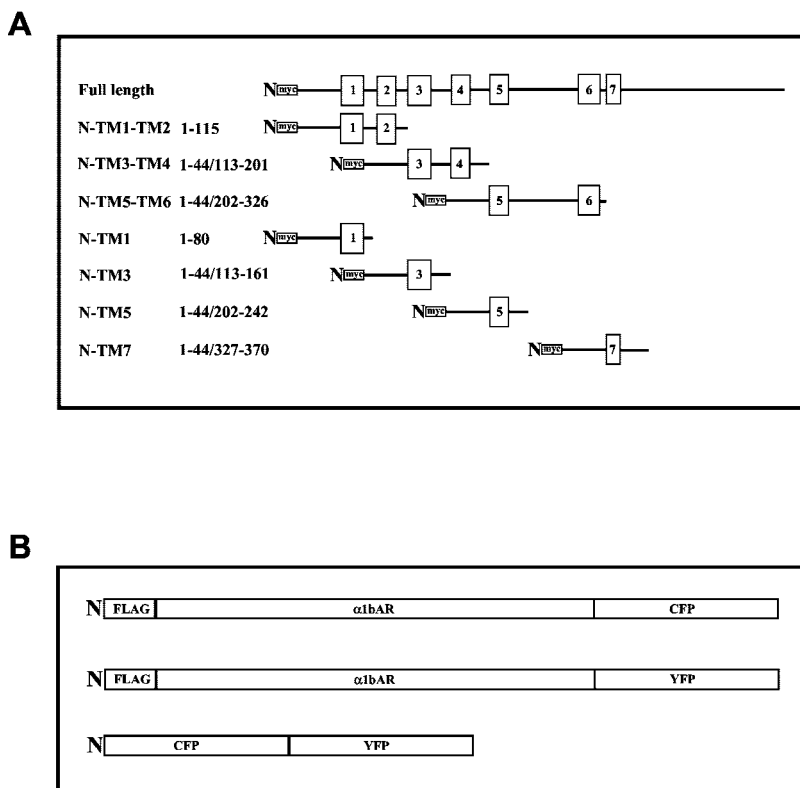
A

B

Fig. 1. Representation of α_{1b}-adrenoceptor fragments and fusion proteins. A, the amino acids of the hamster α_{1b}-adrenoceptor incorporated into the fragments used to explore receptor quaternary structure are shown. B, constructs used for FRET-based studies are illustrated.

fied. Using the amino-terminal primer 5′-TTTCCC<u>AAGCTT</u>ATG-**GAACAAAAACTTATTTCTGAAGAAGATCT**GAATCCCG-ATCTGGACACC-3′, a HindIII restriction site (underlined) followed by an ATG codon and the c-myc tag sequence (bold) was introduced by PCR upstream of the coding sequence of the α$_{1b}$-adrenoceptor. Using the carboxyl-terminal primer 5′-CCG<u>GAAT-TC</u>CCTGGTAACGTCCAGCTGGGG-3′, an EcoRI site was introduced immediately after the 44th amino acid of the N-terminal domain. In the case of the FLAG-tagged constructs, the same strategy was applied but using the amino-terminal primer 5′-TTTCCC**AAGCTTATGGACTACAAGGACGACGATGATA-AG**ATCCCGATCTGGACACC-3′ that introduced a FLAG epitope immediately after the start codon. The amplified fragments were digested with HindIII and EcoRI and subsequently purified.

In the second step, the corresponding TM domains (Fig. 1) of each construct were amplified by PCR, introducing an EcoRI and a KpnI site upstream and downstream of the amplified region, respectively. A stop codon was also introduced after the last codon of the amplified region. The following primers were used (restriction sites are underlined and stop codon in bold): TM3 and TM4: forward, 5′-CCG<u>GAATTC</u>CTGG-GGCGCATCTTCTGTGAC-3′; reverse, 5′-CGG<u>**GGTACC**</u>**CTA**GG-GTTCTTCGGTGACTCCGCA-3′; TM5 and TM6: forward, 5′-CCG-<u>GAATTC</u>TTCTATGCCCTCTTTTCCTCCCTGG-3′; reverse, 5′-CGG<u>**GGTACCCTA**</u>CGGGGGCTTGAGAGTGGAGAAC-3′; and TM7: forward, 5′- CCG<u>GAATTC</u>GACGCCGTGTTCAAGGTGG-TATTC-3′; reverse, 5′-CGG<u>**GGTACCCTA**</u>GCCACTACGGCACT-GGCACC-3′. The amplified fragments were digested with EcoRI and KpnI and purified.

In the last step, the vector pcDNA 3.0 (Invitrogen) was digested with HindIII/KpnI and purified. Then the N-terminal fragment and the amplified sequence of the corresponding TM region were ligated into the vector.

A different strategy was used for the construction of the TM1 and TM1 + TM2 fragment. Using the same amino-terminal primers as those used to amplify the N terminus of the α$_{1b}$-adrenoceptor, either a c-myc or a FLAG tag was introduced immediately after the start codon of the α$_{1b}$-adrenoceptor. Using the carboxyl-terminal primer 5′-AATCGG<u>**GGTACCCTA**</u>GGTGGGCGTCCGCAGGTGCCGAAT-3′, a stop codon (bold) and a KpnI restriction site (underlined) were introduced after the last codon of the amplified region for TM1. Next, the amplified fragment was digested with HindIII/KpnI and ligated into pcDNA3.0. For the construction of TM1 + TM2, the carboxyl-terminal primer 5′-CGGGGTACCCTAGCGCCCCAGAACCCAGTAGC-3′ was used to introduce the KpnI restriction site and the stop codon after the amplified region. Modification of the glycophorin-A–like sequence in both TM1 of the full-length α$_{1b}$-adrenoceptor and the N-TM-1 fragment was produced by standard mutagenesis techniques.

Constructs for Single-Cell FRET. To generate forms of the hamster FLAG α$_{1b}$-adrenoceptor with cyan fluorescent protein (CFP) or enhanced yellow fluorescent protein (eYFP) fused to the C-terminal tail, a FLAGα$_{1b}$-adrenoceptor-Gα$_{11}$ fusion protein described previously (Carrillo et al., 2003) was used as a template. In brief, Gα$_{11}$ was liberated from the fusion construct by digesting with KpnI and NotI. CFP and eYFP were amplified from their original plasmids (BD Biosciences Clontech, Palo Alto, CA) by PCR using the N-terminal primer 5′-CGG<u>GGTACC</u>ATGGTGAGCAAGGGCGAG-GAG-3′, which introduced a KpnI site (underlined) upstream of the coding sequence, and the C-terminal primer 5′-TTTTCCTTTT<u>GCG-GCCGC</u>CTACTTGTACAGCTCGTCCATGCC-3′, which introduced a NotI site after the stop codon. After purification and digestion with KpnI/NotI, both PCR products were ligated into pcDNA3 vector (Invitrogen) containing the α$_{1b}$-adrenoceptor (Fig. 1). FLAGα$_{1b}$-adrenoceptor-eYFP was used to create a CFP-YFP tandem fluorescent protein (Fig. 1). The α$_{1b}$-adrenoceptor was liberated from the original construct by digestion with HindIII/KpnI and subsequently replaced by CFP without the stop codon and flanked by HindIII and KpnI sites. This form of CFP was obtained by PCR using as the N-terminal primer 5′-CCC**AAGCTT**ATGGTGAGCAAGGGCGAGGAG-3′ and a

C-terminal primer 5′-CGG<u>GGTACC</u>CTTGTACAGCTCGTCCAT-GCC-3′.

Transient Transfection of HEK293 Cells. HEK293 cells were maintained in Dulbecco's modified Eagle's medium supplemented with 0.292 g/l L-glutamine and 10% (v/v) newborn calf serum at 37°C in a 5% CO$_2$ humidified atmosphere. Cells were grown to 60 to 80% confluence before transient transfection in 60-mm dishes. Transfection was performed using LipofectAMINE reagent (Invitrogen) according to the manufacturer's instructions.

GPCR Coimmunoprecipitation and Expression Studies. Co-immunoprecipitation studies using FLAG- and c-myc–tagged forms of the full-length α$_{1b}$-adrenoceptor or various fragments of the receptor were performed. Cells were harvested 24 h after transfection and homogenized in 2.5 ml of 1× RIPA buffer (50 mM HEPES, 150 mM NaCl, 1% Triton X-100, and 0.5% sodium deoxycholate) supplemented with 10 mM NaF, 5 mM EDTA, 10 mM NaH$_2$PO$_4$, 5% ethylene glycol, and a protease inhibitor cocktail (Complete; Roche Diagnostics, Indianapolis, IN), pH 7.4, and placed on a rotating wheel at 4°C for 1 h. The samples were then centrifuged for 15 min at 14,000g at 4°C, and the supernatant was transferred to a fresh tube containing 200 μl of 1× RIPA and 50 μl of protein G (Sigma) to preclear the samples. After incubation at 4°C on a rotating wheel for 1 h, the samples were centrifuged at 14000g at 4°C for 1 min, the supernatant was transferred to a fresh tube, and the protein concentration was determined. The protein concentration of individual samples was altered to 1 mg/ml using 1× RIPA and 600 μl of the sample incubated overnight with 40 μl of protein G and 5 μg of M2 anti-FLAG antibody (Sigma) at 4°C on a rotating wheel. A 100-μl sample of the supernatants was reserved to examine protein expres-
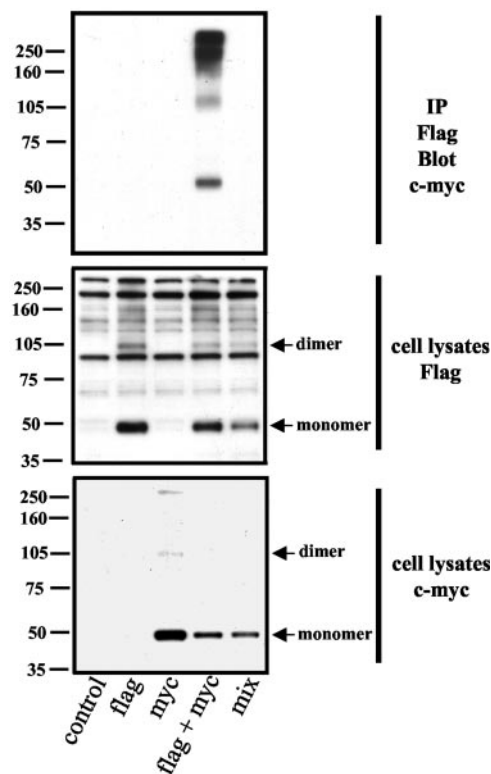

Fig. 2. Coimmunoprecipitation of coexpressed FLAG- and c-myc–tagged forms of the full-length α$_{1b}$-adrenoceptor. FLAG- and c-myc–tagged forms of the full-length α$_{1b}$-adrenoceptor were coexpressed (flag + myc) or expressed individually (flag, myc) in HEK293 cells. Cells individually expressing either the FLAG- or c-myc–tagged forms were also mixed (mix). Cell lysates were generated from both these and untransfected control cells (control). Cell lysates were resolved by SDS-PAGE and immunoblotted to detect either FLAG or c-myc immunoreactivity (bottom) or were immunoprecipitated (IP) with anti-FLAG antibody before SDS-PAGE and immunoblotting to detect c-myc immunoreactivity (top).

sion in the cell lysates and was incubated overnight on a rotating wheel at 4°C. Approximately 16 h later, the samples were centrifuged at 14,000g for 1 min at 4°C, and the protein G beads were washed in 1× RIPA buffer. This was repeated twice more, 40 μl of Laemmli buffer was added, and the samples were heated to 85°C for 4 min. Both immunoprecipitated samples and cell lysates were then subjected to SDS-PAGE analysis using a 4 to 12% Bis-Tris gel (NuPAGE; Invitrogen) and MOPS buffer. After electrophoresis, proteins were transferred onto nitrocellulose membranes that were incubated in 5% milk and 0.1% Tween 20/PBS solution at room temperature on a rotating shaker for 2 h to block nonspecific binding sites. The membrane was incubated with 2.5 μg/μl anti-FLAG antibody overnight in 5% milk and 0.1% Tween 20/PBS at 4°C. Then 16 h later, the membrane was washed three times for 5 min each in 0.1% Tween 20/PBS. Horseradish peroxidase-linked anti-mouse IgG (Amersham Biosciences Inc., Piscataway, NJ) was diluted 1:10,000 in 5% milk, 0.1% Tween 20/PBS was added, and the mixture was incubated for 20 min at room temperature. The membrane was again washed three times in 0.1% Tween 20/PBS before application of enhanced chemiluminescence solution (Pierce Chemical, Rockford, IL) and developing of the immunoblot. Where appropriate, the membrane was subsequently washed using ReBlot Plus solution (Chemicon International, Temecula, CA) diluted 1:10 in H$_2$O for 15 min and then again incubated with 5% milk and 0.1% Tween 20/PBS to block nonspecific sites. The above protocol was repeated with incubation of the membrane with a polyclonal anti–c-myc antibody (Cell Signaling Technology Inc., Beverly, MA) diluted 1:1000 to detect any coimmunoprecipitated material containing the c-myc sequence and detected using a horseradish peroxidase-linked anti-rabbit IgG secondary antibody (Amersham) diluted 1:10,000.

Fluorescent Microscopy and FRET Imaging in Living Cells. An Eclipse TE2000-E (Nikon, Melville, NY) fluorescence inverted microscope was used for living cell microscopy and FRET imaging.

HEK293 cells were grown on polylysine-treated glass coverslips and transiently transfected with the different CFP/eYFP fusion proteins. These coverslips were mounted into a microscope chamber containing physiological saline solution (130 nM NaCl, 5 mM KCl, 1 mM CaCl$_2$, 1 mM MgCl$_2$, 20 mM HEPES, and 10 mM D-glucose, pH 7.4). Images were sequentially obtained in the following order: eYFP, CFP, and FRET filter channels by means of an Optoscan monochromator (Cairn Research, Faversham, Kent, UK) and a dichroic mirror 86002v2bs (Chroma Technology Corporation, Rockingham, VT). The filter sets were the following: eYFP (excitation, 500/5 nm; emission, 535/30 nm); CFP (excitation, 430/12 nm; emission, 470/30 nm); and FRET (excitation, 430/12 nm; emission, 535/30 nm). Illumination time and binning modes were 250 ms and 2 × 2, respectively.

MetaMorph imaging software (Universal Imaging Corporation, West Chester, PA) was used to quantify FRET images by the sensitized FRET method. In brief, corrected FRET (FRET^C) was calculated on a pixel-by-pixel basis for the entire image using the equation FRET^C = FRET − (coefficient B × CFP) − (coefficient A × eYFP), where FRET, CFP, and eYFP corresponded to the background-subtracted images of cells coexpressing CFP and eYFP acquired through the FRET, CFP, and eYFP channels, respectively. B and A correspond to the donor (CFP) and acceptor (eYFP) bleed-through coefficients, respectively, and they were calculated from cells expressing only CFP- or eYFP-containing proteins. In the present set of experiments, we obtained the following values for each coefficients: B = 0.65, and A = 0.20.

To normalize FRET^C values according to the different expression levels of donor (CFP) and acceptor (eYFP) proteins, we used the equation FRET^N = FRET^C/CFP× eYFP, where FRET^C, CFP, and eYFP are the fluorescent values, after background subtraction, obtained from selected cells. To validate this technique, we used cells expressing the tandem fluorescent protein (CFP-eYFP) as a positive control, and as a negative control we used cells coexpressing both
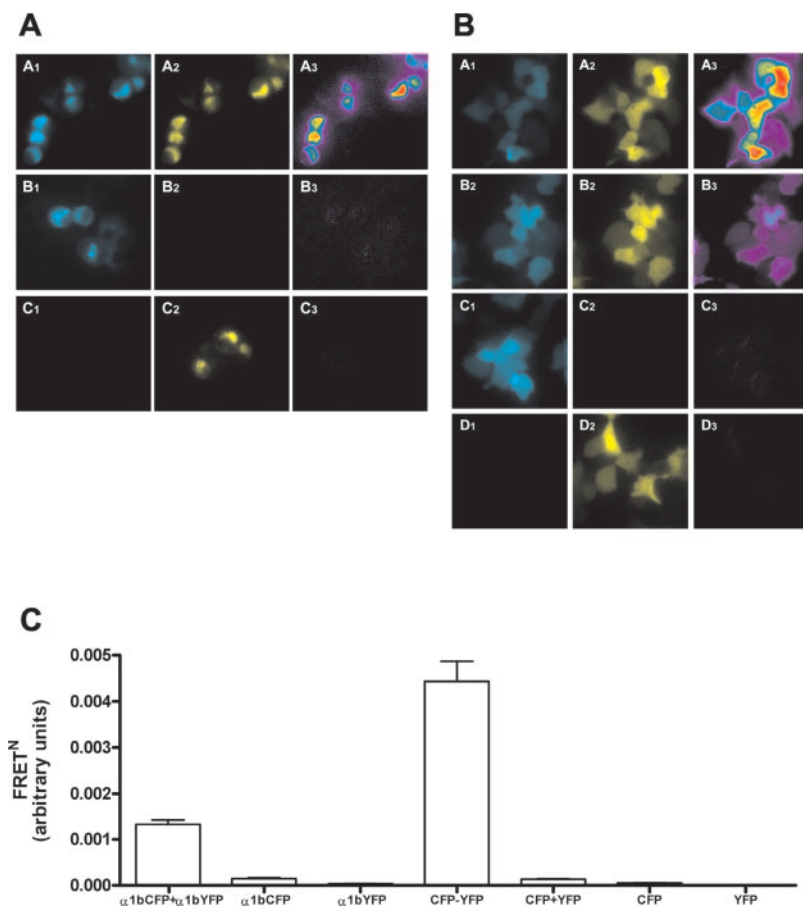

Fig. 3. Single-cell FRET studies detect interactions between CFP- and eYFP-tagged forms of the α_{1b}-adrenoceptor. A, forms of the α_{1b}-adrenoceptor C-terminally tagged with either CFP or eYFP were coexpressed (A$_1$–A$_3$) or individually (CFP, B$_1$–B$_3$; eYFP, C$_1$–C$_3$) in HEK293 cells. CFP (as energy donor) was detected using the filter set at excitation 430 nm and emission 470 nm (A$_1$, B$_1$, and C$_1$), and eYFP (as energy acceptor) with the filter set at excitation 500 nm and emission 535 nm (A$_2$, B$_2$, and C$_2$). Corrected FRET signals (see *Materials and Methods*) are displayed in A$_3$, B$_3$, and C$_3$. B, a FRET-positive control in which CFP and eYFP are produced in a single open-reading frame was expressed in HEK293 cells (A$_1$–A$_3$). CFP and eYFP were coexpressed (B$_1$–B$_3$) or were expressed individually (CFP, C$_1$–C$_3$; eYFP, D$_1$–D$_3$). Expression (A$_1$–D$_1$, A$_2$–D$_2$) and corrected FRET (A$_3$–D$_3$) were detected as in 3A. C, corrected FRET corresponding to images akin to those in 3A and 3B was quantified.

CFP and eYFP proteins or cells only expressing donor (CFP) and acceptor (eYFP) proteins (see *Results* for details).

Time-Resolved Fluorescence Resonance Energy Transfer. Time-resolved fluorescence resonance energy transfer was performed on intact HEK293 cells using Eu^{3+}-labeled anti–c-myc antibodies and allophycocyanin-labeled anti-FLAG antibodies as described by McVey et al. (2001).

Data Analysis. All experiments were performed on at least three independent occasions. Where appropriate, data are presented as means ± S.E.M.

Results

Forms of the hamster α_{1b}-adrenoceptor were generated that incorporated either the c-myc or the FLAG epitope tag at the extreme N terminus. These were expressed either individually or in combination in HEK293 cells. Immunoblotting SDS-PAGE–resolved lysates of these cells with either anti–c-myc or anti-FLAG antibodies resulted in detection of polypeptides of approximately 50 kDa in the appropriate positively transfected cells but not in lysates of mock-transfected cells or of those transfected only with the alternate construct (Fig. 2). A relatively small fraction of the specific anti–c-myc and anti-FLAG immunoreactivity in such SDS-PAGE cell lysates migrated with apparent mass of approximately 100 kDa, suggesting the possibility that some of the α_{1b}-adrenoceptor was present as an SDS-resistant dimer (Fig. 2). Particularly in the anti–c-myc immunoblots, a further immunoreactive species with higher apparent molecular mass was also detected. Immunoprecipitation, using anti-FLAG antibodies, of lysates of cells transfected to coexpress the c-myc–and FLAG-tagged forms of the α_{1b}-adrenoceptor resulted in coimmunoprecipitation of anti–c-myc immunoreactivity. In SDS-PAGE gels of such immunoprecipitated material, anti–c-myc immunoreactivity was detected as a mixture of a 50-kDa polypeptide and a band of approximately 100 kDa of the size anticipated for a receptor dimer. The strongest signals, however, corresponded to a series of less rapidly migrating species that may represent higher-order oligomers or other quaternary structures (Fig. 2). Coimmunoprecipitation of c-myc immunoreactivity was not produced when either the c-myc–or the FLAG-tagged forms of the α_{1b}-adrenoceptor were expressed individually or when cell lysates expressing either the c-myc–or the FLAG-tagged forms of the receptor were combined before immunoprecipitation (Fig. 2). Such observations are consistent with dimerization/oligomerization between the coexpressed, differentially tagged forms of the α_{1b}-adrenoceptor (Carrillo et al., 2003). Because GPCR immunoprecipitation studies require dissolution of cellular structure and membrane integrity, we also wished to demonstrate interactions of differentially modified forms of the α_{1b}-adrenoceptor in intact cells. The α_{1b}-adrenoceptor was thus tagged at the C terminus with either CFP or eYFP. Both of these constructs were successfully expressed in HEK293 cells (Fig. 3A). As observed with heterologous expression of many GPCRs, a substantial fraction of these two constructs was located in the perinuclear region of individual cells (Fig. 3A). After coexpression of α_{1b}-adrenoceptor-CFP and α_{1b}-adrenoceptor-eYFP, corrections to eliminate apparent FRET signals generated because of the overlapping spectral characteristics of CFP and eYFP allowed detection and quantitation of corrected FRET between these constructs in single, individual cells (Fig. 3, A and C). In contrast, coexpression of CFP and eYFP did not result in a substantial FRET signal (Fig. 3, B and C), although a fusion protein in which CFP and eYFP were expressed as a single polypeptide did result in a strong FRET signal (Fig. 3, B and C). These results confirmed that the FRET signal produced by coexpression of α_{1b}-adrenoceptor-CFP and α_{1b}-adrenoceptor-eYFP did not reflect significant mutual affinity between the two fluorescent proteins but did require their proximity. The distance constraints of FRET (Eidne et al., 2002; Milligan, 2004b) are thus also consistent with the α_{1b}-adrenoceptor existing within a dimeric or oligomeric complex. To assess whether at least a fraction of expressed α_{1b}-adrenoceptor constructs was delivered to the cell surface of HEK293 cells, we used TR-FRET in intact HEK293 cells (McVey et al., 2001; Ramsay et al., 2004). The N-terminally c-myc–and FLAG-tagged forms of the α_{1b}-adrenoceptor were expressed either individually or in combination. Both intact cotransfected cells and mixtures of cells expressing either of the two constructs were exposed to a combination of europium-labeled anti–c-myc antibodies as energy donor and allophycocyanin (APC)-labeled anti-FLAG antibodies as energy acceptor. After excitation at 330 nm, a
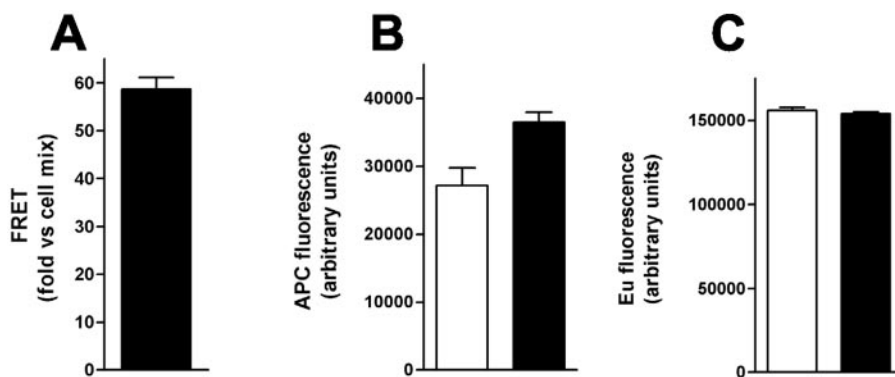

Fig. 4. TR-FRET detects α_{1b}-adrenoceptor interactions at the surface of HEK293 cells. N-terminally FLAG- and c-myc–tagged forms of the α_{1b}-adrenoceptor were expressed individually or were coexpressed in HEK293 cells. Cells expressing the two forms of the receptor were mixed, and these as well as the cotransfected cells were exposed to a combination of europium-labeled anti–c-myc antibodies as energy donor and APC-labeled anti-FLAG antibodies as energy acceptor. A, time-resolved FRET was measured and is presented as the fold signal from cotransfected cells compared with the mixed cell population. To confirm equivalent cell-surface expression of the two forms of the α_{1b}-adrenoceptor in the cotransfected and mixed cells, fluorescence corresponding to binding to the energy acceptor (FLAG-tagged receptor) (B) and the energy donor (c-myc–tagged receptor) (C) was measured in the mixed (□) and cotransfected (■) cells.

strong output at 665 nm consistent with FRET was observed from the cells coexpressing the two forms of the receptor, and this was approximately 60-fold greater than signals obtained from the mixed population of cells (Fig. 4A). This did not reflect poor expression of either the FLAG- or c-myc–tagged form of the α_{1b}-adrenoceptor in the cells individually transfected and then mixed. Direct monitoring of the fluorescence associated with APC-labeled anti-FLAG and europium-labeled anti–c-myc antibodies bound to cells indicated equivalent levels of cell-surface α_{1b}-adrenoceptors in the cotransfected and mixed cell populations (Fig. 4, B and C).

Previous studies have suggested a role for TM1 in producing the quaternary structure of the α_{1b}-adrenoceptor (Carrillo et al., 2003; Stanasila et al., 2003). To assess this further, FLAG- and c-myc–tagged forms of the N-terminal extracellular region of the receptor linked to the sequence defining TM1 were generated (N-TM1). These incorporated amino acids 1 to 80 of the α_{1b}-adrenoceptor (Fig. 1). Immunoblotting of appropriate cell lysates confirmed expression of these constructs as approximately 12-kDa polypeptides (Fig. 5A, left). Immunoprecipitation using anti-FLAG antibodies resulted in pull-down of anti-FLAG immunoreactivity from lysates expressing the FLAG N-TM1 construct in isolation, those coexpressing FLAG N-TM1 and c-myc N-TM1, and lysates individually expressing either FLAG N-TM1 or c-myc N-TM1 that was mixed before performing the immunoprecipitation (Fig. 5A, right). Coimmunoprecipitation of the c-

myc N-TM1 fragment was produced when the anti-FLAG immunoprecipitations were performed on lysates of cells coexpressing the c-myc and FLAG forms of N-TM1 but not after combination of lysates expressing each construct separately (Fig. 5A, right). Such results are consistent with self-association *of* N-TM1 and a potential role of this region in producing quaternary structure. In addition to the detection of the 12-kDa c-myc N-TM1 fragment in the anti-FLAG immunoprecipitates from lysates of cells coexpressing the differentially epitope-tagged forms of N-TM1, a band of approximately twice this size was also present. This is probably an SDS-resistant dimer of the N-TM1 fragment because it was not present unless the lysates were from cells coexpressing the two forms of the N-TM1 fragment (Fig. 5A). Studies on the TM1 segment of the *Saccharomyces cerevisiae* α factor receptor have indicated a key role of the **GXXXG** glycophorin-A dimerization-like sequence in TM1 of this receptor in generation of quaternary structure (Overton et al., 2003). It has also been suggested that the affinity of interaction between such motifs is modulated by the contribution of more distant contacts (Melnyk et al., 2004). The hamster α_{1b}-adrenoceptor has a similar sequence within TM1, with a Leu residue located a further turn of the helix below the second glycine ($G^{49}LVLG^{53}FRIL^{57}$). We modified this sequence within the c-myc N-TM1 construct to $L^{49}LVLL^{53}FRIA^{57}$ (the LLA mutant). This construct was also expressed as a 12-kDa polypeptide (Fig. 5B). When coexpressed with FLAG N-TM1
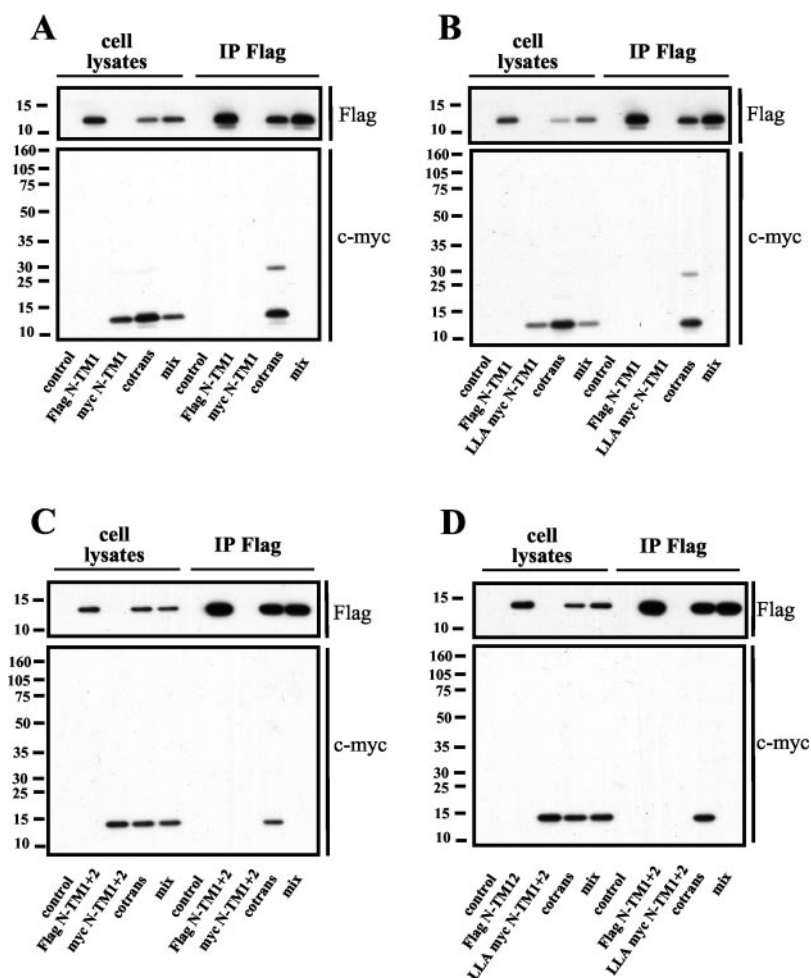

Fig. 5. Self-association of α_{1b}-adrenoceptor fragments containing TM1: lack of importance of the glycophorin-A–like motif. FLAG-tagged N terminus plus TM1 of the α_{1b}-adrenoceptor (Flag N-TM1) (A and B) or FLAG-tagged N terminus plus TM1 + TM2 (Flag N-TM1 + TM2) (C and D) were expressed individually or along with c-myc–tagged N terminus plus TM1 (A), the mutated glycophorin-A–like (LLA) version of this construct (B), c-myc–tagged N terminus plus TM1 + TM2 (C), or the LLA version of this construct (D). Cell lysates generated from these cells, from mixed populations of cells expressing the constructs individually, and from non-transfected control cells were resolved by SDS-PAGE and immunoblotted to detect either FLAG or c-myc immunoreactivity (left of each) or were immunoprecipitated with anti-FLAG antibody (right of each) before SDS-PAGE and then immunoblotted to detect either FLAG or c-myc immunoreactivity.

and immunoprecipitation performed with anti-FLAG antibodies, c-myc N-TM1 LLA was coimmunoprecipitated as effectively as the wild-type c-myc N-TM1 fragment (Fig. 5B), suggesting that this region does not play a key role in TM1 self-association and hence in producing quaternary structure in this receptor. The antiparallel orientation of the odd- and even-numbered TM helices of GPCRs means that it was not possible to generate FLAG- and c-myc–tagged forms of the N-terminal region linked directly to the even-numbered TM segments. To overcome this, we next examined the expression and potential interactions of FLAG- and c-myc–tagged N-TM1 + TM2, in which the first intracellular loop was maintained to link together TM1 and TM2 (Fig. 1). These constructs thus incorporated amino acids 1 to 115 of the receptor. Both c-myc N-TM1 + TM2 and FLAG N-TM1 + TM2 were detected as 14-kDa polypeptides (Fig. 5C). As with the N-TM1 constructs, coexpression of c-myc N-TM1 + TM2 and FLAG N-TM1 + TM2 allowed and was required for their

coimmunoprecipitation (Fig. 5C). Coexpression of FLAG N-TM1 + TM2 with c-myc N-TM1 + TM2 containing the disrupted LLA, glycophorin-A dimerization-like sequence also did not inhibit coimmunoprecipitation (Fig. 5D).

c-myc–tagged forms of each of the full-length α_{1b}-adrenoceptors and of N-TM1 + TM2, N-TM3 + TM4, N-TM5 + TM6, and N-TM7 were expressed individually in HEK293 cells, and after fixation, expression, and distribution of these constructs, they were assessed by immunocytochemistry (Fig. 6A). All were expressed with a similar pattern with a substantial level of intracellular, perinuclear staining. To assess whether N-TM1 + TM2 was able to interact with the full-length α_{1b}-adrenoceptor, the FLAG-tagged α_{1b}-adrenoceptor was coexpressed with c-myc N-TM1 + TM2. Immunoblotting studies on cell lysates confirmed expression of the 50-kDa FLAG-α_{1b}-adrenoceptor (Fig. 6B, top left) and the 14-kDa c-myc N-TM1 + TM2 (Fig. 6B, bottom left). Immunoprecipitation with anti-FLAG antibodies successfully
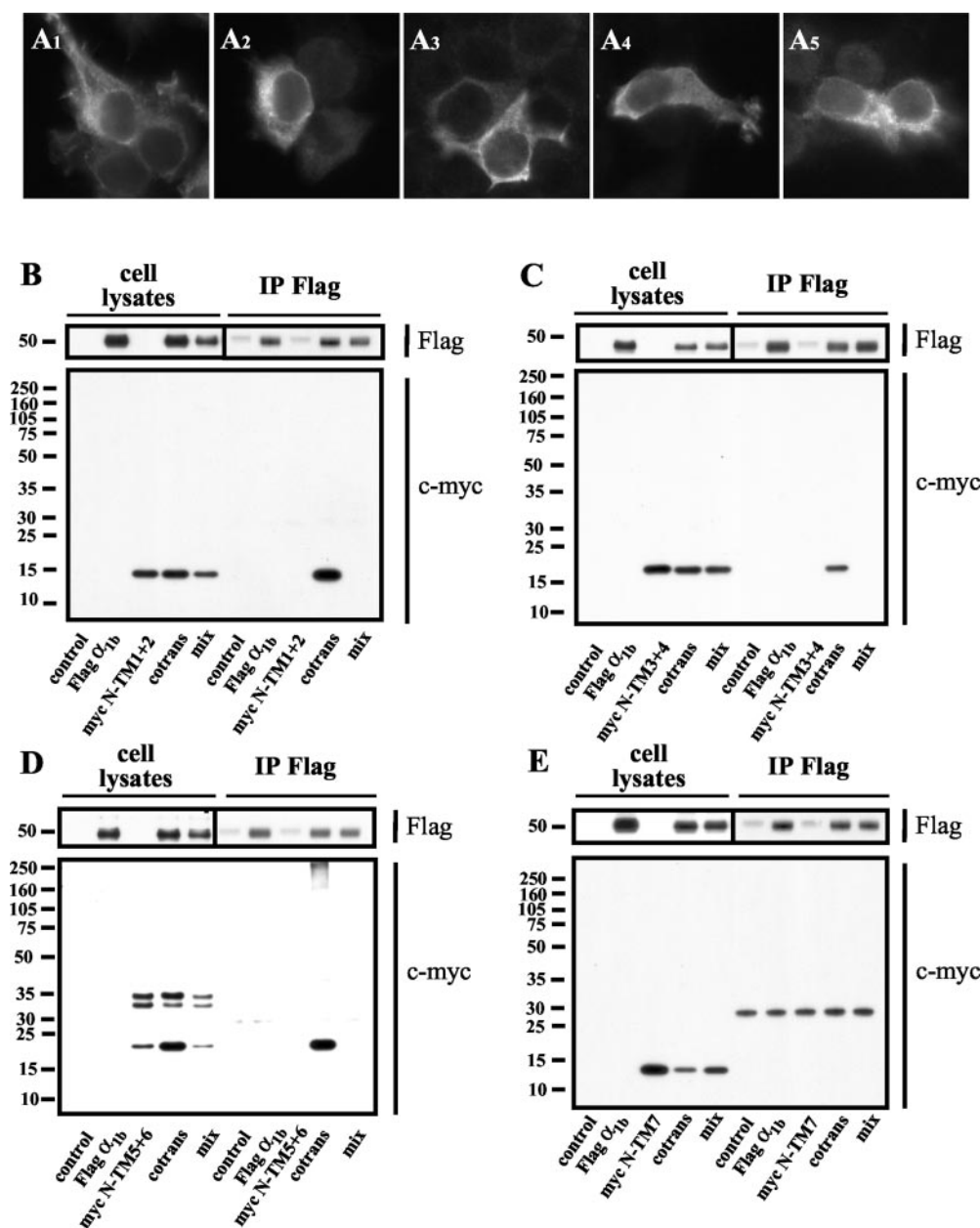

Fig. 6. Interactions between fragments of the α_{1b}-adrenoceptor and the full-length receptor. The FLAG-tagged full-length α_{1b}-adrenoceptor (A$_1$, B–E) and c-myc–tagged fragments in which the N-terminal extracellular domain was linked to TM1 + TM2 (A$_2$ and B), TM3 + TM4 (A$_3$ and C), TM5 + TM6 (A$_4$ and D), and TM7 (A$_5$ and E) were either expressed individually or coexpressed in HEK293 cells. A, cells were fixed and immunostained with anti–c-myc antibody. Cell lysates akin to those of Fig. 5 were resolved by SDS-PAGE or first immunoprecipitated (IP) with anti-FLAG antibody and then immunoblotted to detect either FLAG or c-myc immunoreactivity. The nonspecifically labeled band of approximately 30 kDa observed in all lanes of the immunoprecipitations in E probably represents the light chain of the anti-FLAG antibody. This was usually observed only when development of the immunoblots was sustained in attempts to detect a small extent of coimmunoprecipitation.

pulled down FLAG-α_{1b}-adrenoceptor from all lysates in which it was expressed (Fig. 6B, top right). In all cases, immunoprecipitation of cell lysates with anti-FLAG antibodies followed by immunoblotting of the SDS-PAGE–resolved lysates with the same anti-FLAG antibodies resulted in weak detection of a polypeptide of approximately 52 kDa. This is presumably the heavy chain of the anti-FLAG antibody. Co-immunoprecipitation of c-myc N-TM1 + TM2 was achieved only from lysates of cells in which it was coexpressed with the FLAG-α_{1b}-adrenoceptor (Fig. 6B, bottom right). To extend these studies, FLAG-α_{1b}-adrenoceptor was coexpressed with c-myc N-TM3 + TM4 (Fig. 6C), c-myc N-TM5 + TM6 (Fig. 6D), or c-myc N-TM7 (Fig. 6E). In each case, immunoblotting of cell lysates confirmed the anticipated pattern of expression of both the FLAG-α_{1b}-adrenoceptor and the c-myc–tagged fragments. Each of the receptor fragments, with the exception of c-myc N-TM5 + TM6, migrated as a single polypeptide of the anticipated size (Fig. 6, C–E). c-myc N-TM5 + TM6 produced a more complex immunostaining pattern with two extra distinct bands of apparent molecular mass between 33 and 35 kDa. Although reminiscent of patterns associated with differential glycosylation, the basis and significance of this were not investigated in detail. For both c-myc N-TM3 + TM4 (Fig. 6C) and c-myc N-TM5 + TM6 (Fig. 6D), coexpression with the FLAG-α_{1b}-adrenoceptor resulted in coimmunoprecipitation of these fragments with the full-length receptor. These were not nonspecific interactions because, although coexpression of c-myc N-TM7 with the FLAG-α_{1b}-adrenoceptor could be shown (Fig. 6E) with similar cellular distribution (Fig. 6A), immunoprecipitation of the FLAG-α_{1b}-adrenoceptor did not result in coimmunoprecipitation of c-myc N-TM7 (Fig. 6E). The ability of three distinct segments

of the α_{1b}-adrenoceptor to interact with the full-length receptor cannot be explained easily by a simple dimeric structure defined by a single set of contacts. Such results suggest that the in vivo organization of the α_{1b}-adrenoceptor may represent an oligomeric complex.

Interactions between the receptor fragments and the full-length α_{1b}-adrenoceptor at the cell surface were explored by TR-FRET. Cells were cotransfected with the full-length FLAG-α_{1b}-adrenoceptor and each of c-myc N-TM1 + TM2, c-myc N-TM3 + TM4, and c-myc N-TM5 + TM6. A substantial TR-FRET signal was obtained compared with that observed upon addition of the antibodies to mixtures of cells individually expressing FLAG-α_{1b}-adrenoceptor or the receptor fragments (Fig. 7A). These results confirmed cell-surface delivery of each of these three receptor fragments and are consistent with interactions of each fragment with the full-length receptor at the cell surface. When calculated as a fold FRET signal produced in cells coexpressing the constructs compared with the signal from mixed populations of cells each expressing a single construct, N-TM1 + TM2 and N-TM3 + TM4 generated substantially greater signals than did N-TM5 + TM6 (Fig. 7A).

Such differences in signal are, however, difficult to interpret because FRET-based assays are sensitive to both the distance between and the relative orientation of the energy donor and acceptor species (Milligan, 2004b). However, TR-FRET signals produced by coexpression of c-myc N-TM1 + TM2 or c-myc N-TM3 + TM4 with the FLAG full-length receptor were substantially lower than after coexpression of the FLAG- and c-myc–tagged full-length receptors (Fig. 7A). Accepting the caveat noted above, this is at least consistent with the hypothesis that intermolecular contacts from more
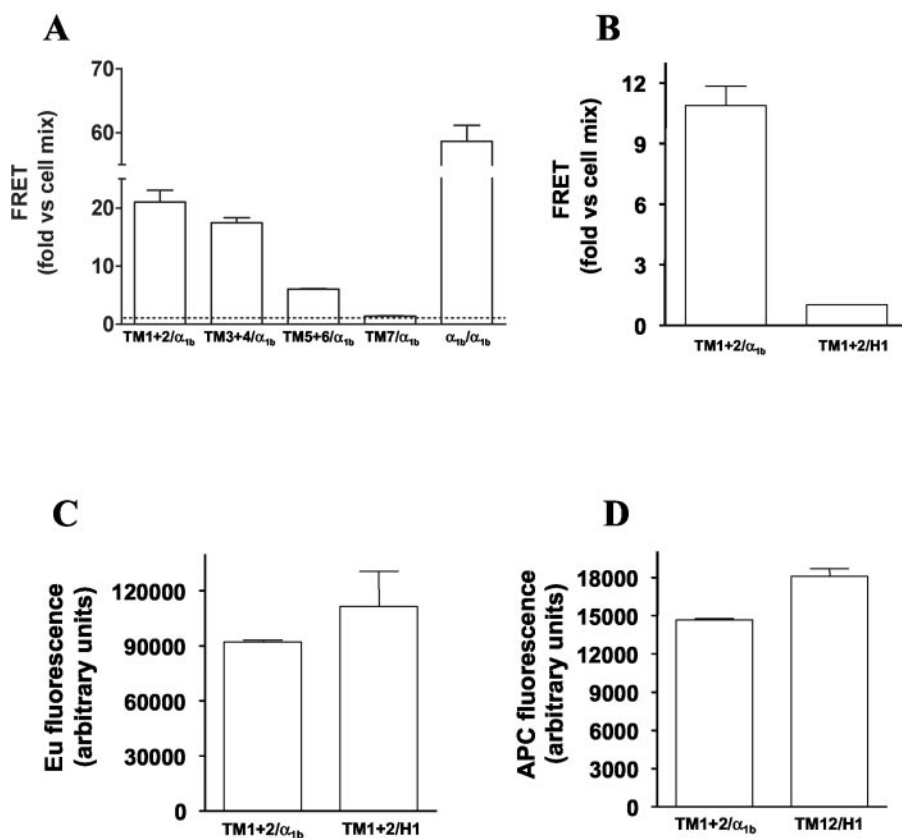

Fig. 7. TR-FRET detects selective cell-surface interactions of the α_{1b}-adrenoceptor with a number of receptor fragments. A, TR-FRET was measured as in Fig. 3 after coexpression of the FLAG-tagged α_{1b}-adrenoceptor and c-myc–tagged fragments in which the N-terminal extracellular domain was linked to TM1 + TM2, TM3 + TM4, TM5 + TM6, or TM7. Parallel studies were performed in mixed populations of cells in which the c-myc–and FLAG-tagged constructs were expressed individually. The TR-FRET signal produced after expression of FLAG and c-myc–tagged forms of the full-length receptor are also shown. B–D, c-myc TM1 + TM2 of the α_{1b}-adrenoceptor (TM12) was coexpressed with N-terminally FLAG-tagged forms of either the α_{1b}-adrenoceptor (α_{1b}) or the histamine H1 receptor (H1), or cells expressing these constructs individually were mixed. B, TR-FRET was measured after the addition of both Eu^{3+}-labeled anti–c-myc antibodies and APC-labeled anti-FLAG antibodies. Cell-surface expression of c-myc TM1 + TM2 (C) and FLAG α_{1b}-adrenoceptor and FLAG histamine H1 receptor (D) in cotransfected cells was monitored via binding of appropriate antibodies.

than one part of the receptor are required to produce the full oligomeric structure. Although c-myc N-TM7 could clearly be expressed (Fig. 6), direct monitoring of europium fluorescence upon the addition of labeled anti–c-myc antibodies to intact cells indicated little of this fragment to be delivered to the cell surface (data not shown).

A key issue in any study of protein-protein interactions using either fragments or full-length forms of transmembrane polypeptides is to provide relevant and convincing negative controls. We have indicated previously that interactions can occur between the α_{1b}-adrenoceptor and the histamine H1 receptor but that these are of low affinity compared with α_{1b}-adrenoceptor homodimeric interactions (Carrillo et al., 2003). We therefore either coexpressed c-myc N-TM1 + TM2 of the α_{1b}-adrenoceptor along with an N-terminally FLAG-tagged form of the full-length human histamine H1 receptor or expressed these constructs in individual cell populations that were subsequently mixed. In contrast to data obtained after expression of c-myc N-TM1 + TM2 with FLAG-full-length α_{1b}-adrenoceptor, addition of a combination of Eu^{3+}-labeled anti–c-myc antibodies and APC-labeled anti-FLAG antibodies did not result in any higher level of energy transfer signal from cells in which the two constructs were coexpressed (Fig. 7B). This was not a reflection that cell-surface delivery of the c-myc N-TM1 + TM2 fragment of the α_{1b}-adrenoceptor was not achieved in cells coexpressing the histamine H1 receptor (Fig. 7C) or that the histamine H1 receptor was expressed more poorly at the cell surface than the full-length α_{1b}-adrenoceptor (Fig. 7D).

We next assessed potential interactions between epitope-tagged fragments of the α_{1b}-adrenoceptor, because previous studies have shown that coexpressed fragments of a GPCR can reconstitute structure and function (Martin et al., 1999; Overton and Blumer, 2002) and can therefore presumably interact. Interactions between N-TM1 + TM2 and N-TM3 + TM4 were essentially undetectable after their coexpression, whether FLAG N-TM1 + TM2 was used to attempt to coimmunoprecipitate c-myc N-TM3 + TM4 or the protocol was reversed and FLAG N-TM3 + TM4 was immunoprecipitated in the presence of coexpressed c-myc N-TM1 + TM2 (Fig. 8). In each case, both constructs were expressed, and the anti-FLAG antibodies successfully immunoprecipitated the FLAG-tagged fragment (Fig. 8). FLAG N-TM1 + TM2 also showed no propensity to interact with c-myc N-TM7 (Fig. 9A). Likewise, c-myc N-TM7 was unable to be coimmunoprecipitated with coexpressed FLAG N-TM3 + TM4 or FLAG N-TM5 + TM6 (Fig. 9, B and C). These results and the lack of interaction of N-TM7 with the full-length receptor (Fig. 6D) do not suggest an important role of TM7 in α_{1b}-adrenoceptor homodimerization/oligomerization and stand somewhat in contrast to the data of Stanasila et al. (2003). In a similar vein, coexpression of N-TM3 + TM4 with N-TM5 + TM6 did not allow their coimmunoprecipitation, whether the FLAG-tagged form used for the immunoprecipitation was N-TM3 + TM4 or N-TM5 + TM6 (Fig. 10). Like N-TM1 + TM2, N-TM3 + TM4 was able to self-associate (Fig. 11A). To assess the contribution of TM3, we coexpressed c-myc N-TM3 + TM4 along with FLAG N-TM3 (Fig. 1). FLAG N-TM3 was expressed and successfully immunoprecipitated by the anti-FLAG antibodies, but no coimmunoprecipitation of c-myc N-TM3 + TM4 was now observed (Fig. 11B). These results indicate that TM3 was not responsible for coimmunoprecipi-

tation of coexpressed FLAG and c-myc–tagged forms of N-TM3 + TM4 and hence imply a key role for either TM4 or, possibly, the amino acids of intracellular loop 2 that link TM segments 3 and 4. No self-association of N-TM5 + TM6 was noted in equivalent immunoprecipitation studies (Fig. 11C). These results were supported by TR-FRET–based studies in which a strong signal was obtained after coexpression of FLAG and c-myc forms of N-TM3 + TM4. However, no significant TR-FRET signals consistent with cell-surface interactions between N-TM1 + TM2 and N-TM3 + TM4 or between N-TM3 + TM4 and N-TM5 + TM6 could be recorded (Fig. 12). Finally, we were able to observe both coimmunoprecipitation of (Fig. 13A) and cell surface TR-FRET between (Fig. 13B) N-TM5 + TM6 and N-TM1 + TM2 when these constructs were coexpressed. A summary of these interac-
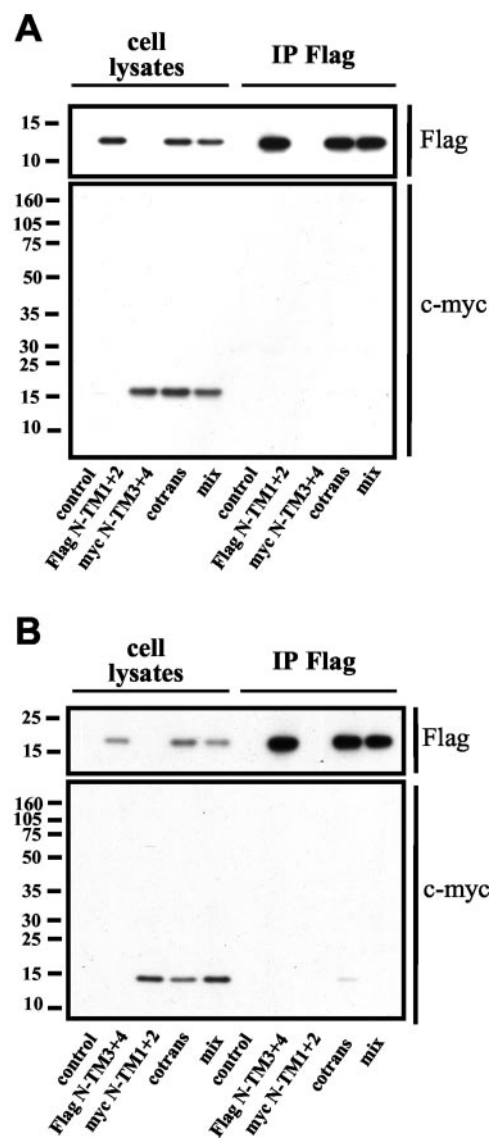

Fig. 8. Lack of interactions between TM1 + TM2 and TM3 + TM4. FLAG- (A) or c-myc (B)-tagged forms of the N terminus and TM1 + TM2 and c-myc–(A) or FLAG (B)-tagged forms of the N terminus and TM3 + TM4 were expressed individually or in combination. Expression of these constructs was monitored in cell lysates as described in Fig. 6, and the capacity of anti-FLAG antibodies to immunoprecipitate the FLAG-tagged constructs was monitored. Although immunoprecipitation was effective, interactions between N-TM1 + TM2 and N-TM3 + TM4 were not observed because they were not coimmunoprecipitated.

tions is provided in Table 1. Although not performed as extensively as the coimmunoprecipitation studies, the pattern of positive interactions of these fragments at the cell surface, monitored by TR-FRET, was entirely consistent with the immunoprecipitation studies (Table 1).

These data clearly implicate central roles for TM1 (and possibly TM2) and the TM4 segment (or possibly intracellular loop 2) in providing interactions that contribute to the quaternary structure of the α_{1b}-adrenoceptor, with symmetrical contacts between the TM1 and the TM4 regions likely to be important. The data are also consistent with contributions of the TM5 + TM6 region. However, a lack of symmetrical interactions for this region may implicate it as more relevant to interdimer contacts that contribute to organization of higher oligomeric structure.

Discussion

Production of the functional GABAb receptor requires coexpression of the protein products of two distinct GPCR genes (White et al., 1998). Evidence of direct protein-protein interactions involving the C-terminal tails of these proteins, that this interaction masked an endoplasmic reticulum retention motif and hence allowed cell-surface delivery of the complex, and that only the GABAbr1 subunit was able to

bind the neurotransmitter GABA, provided clear evidence for the heterodimeric structure of the functional receptor. Parallel studies on the structure of the extracellular domain of the metabotropic glutamate receptor 1a provided direct structural evidence of dimerization (Kunishima et al., 2000). These receptors belong to the small group of family 3 GPCRs that all have long N-terminal extracellular elements in which the ligands bind (Parmentier et al., 2002). Considerable evidence also indicates that members of the large family of rhodopsin-like class 1 GPCRs also have quaternary structure (George et al., 2002; Milligan et al., 2003; Milligan, 2004a). However, the majority of these studies have used techniques that cannot discriminate between GPCR dimers and the presence of GPCRs within higher-order oligomers. Protein refolding studies indicate that the leukotriene B4 BLT1 receptor can form a dimer (Baneres and Parello, 2003) and that dimeric structure is the basic requirement to bind a single heterotrimeric G protein (Baneres and Parello, 2003). Application of atomic-force microscopy has shown the presence of apparent rhodopsin dimers in murine rod outer segments, confirming their presence in physiological settings, but these studies also detected further organization and structure with rows, or arrays, of dimers being aligned (Liang et al., 2003). It might be argued that the high concentration and special-
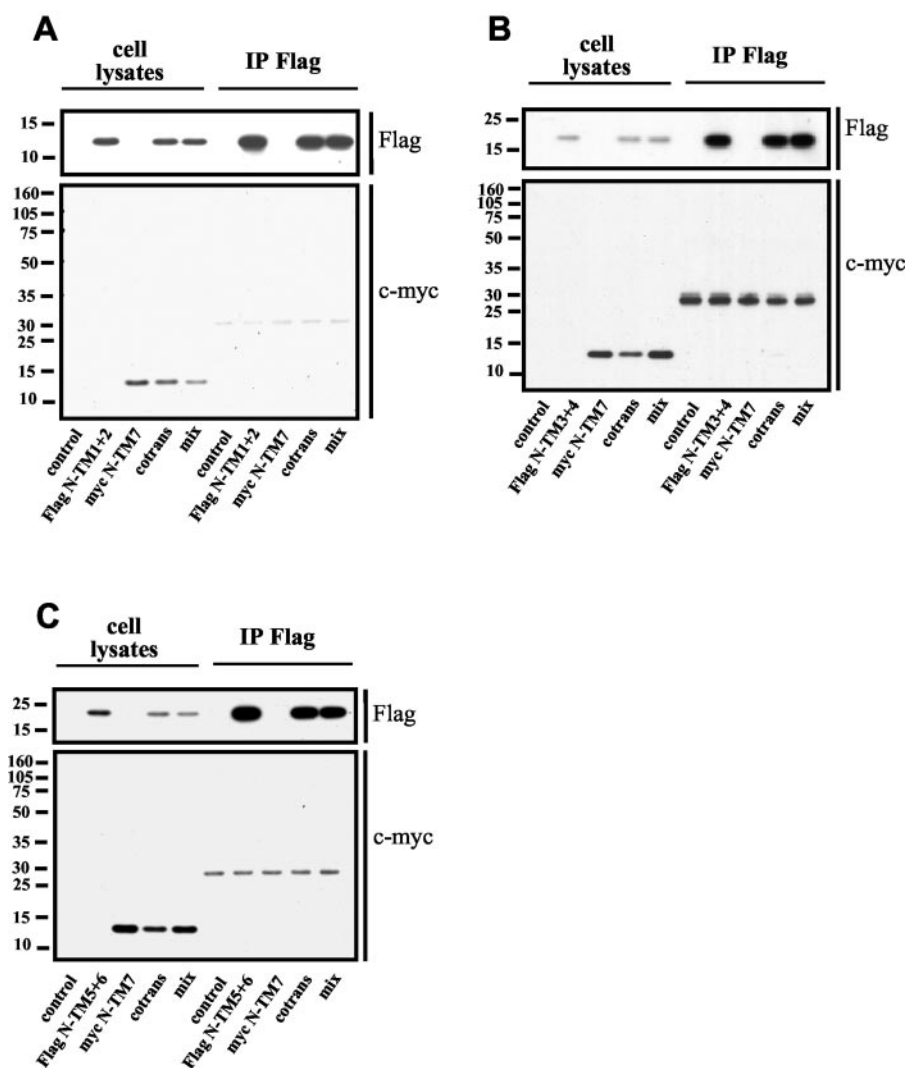

Fig. 9. TM7 of the α_{1b}-adrenoceptor does not interact with any other TM segment. FLAG-tagged forms of N-TM1 + TM2 (A), N-TM3 + TM4 (B), or N-TM5 + TM6 were expressed in isolation or in combination with c-myc N-TM7. Immunoblotting and immunoprecipitation (IP) studies confirmed expression of all constructs in the appropriate cell lysates, but c-myc N-TM7 was not coimmunoprecipitated with any of the FLAG-tagged fragments.

ized function of rhodopsin in rod outer segments would generate and require specific organization beyond other GPCRs. However, recent studies on the complement C5a receptor that examined cross-linking between forms of this protein into which cysteine residues had been engineered at specific locations concluded that the receptor may exist within higher order oligomers or in clusters (Klco et al., 2003). These conclusions were largely derived from the data being inconsistent with a simple, single symmetrical interface model and with other studies suggesting distinct models of dimerization. As noted by Klco et al. (2003), it is clearly possible that different members of the GPCR family have evolved different mechanisms to produce homodimers. This may well be the case for family 1 compared with family 3 receptors because they have evolved entirely separately. However, although informatic studies provide hypotheses to suggest that even very closely related GPCRs may have quite distinct mechanisms of homodimerization (Filizola and Weinstein, 2002), this is perhaps surprising given the parsimonious adaptation
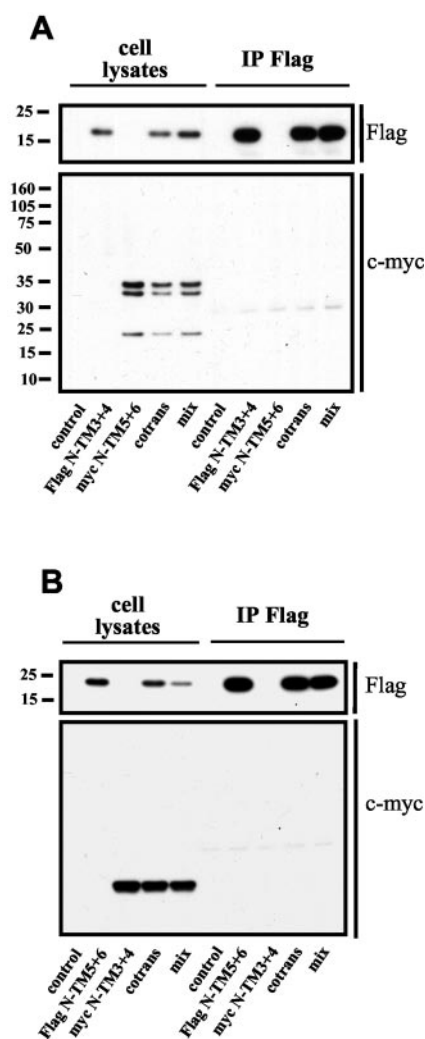
Fig. 10. Lack of interactions between TM3 + TM4 and TM5 + TM6. FLAG- (A) or c-myc (B)-tagged forms of N-TM3 + TM4 and c-myc–(A) or FLAG (B)-tagged forms of N-TM5 + TM6 were expressed individually or in combination. Expression of these constructs was monitored in cell lysates as described in Fig. 6, and the capacity of anti-FLAG antibodies to immunoprecipitate (IP) the FLAG-tagged constructs was monitored. Although immunoprecipitation was effective, interaction between N-TM3 + TM4 and N-TM5 + TM6 was not observed.
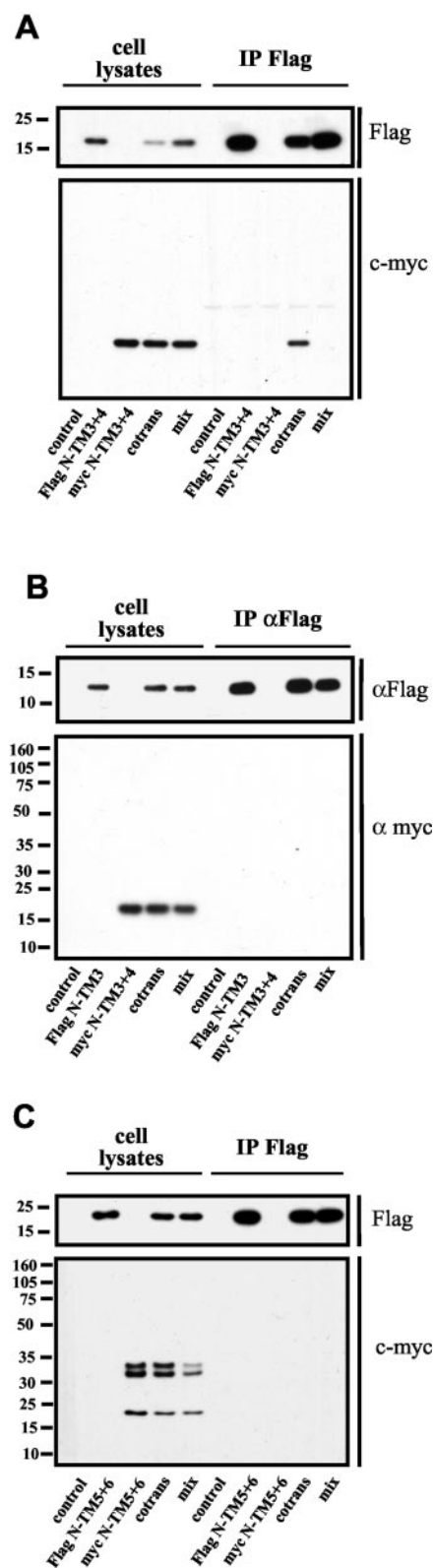
Fig. 11. Self-association of TM4 but not TM5 + TM6. FLAG- and c-myc–tagged forms of N-TM3 + TM4 (A), FLAG N-TM3 and c-myc N-TM3 + TM4 (B), and FLAG- and c-myc–tagged forms of N-TM5 + TM6 (C) were expressed individually or in combination. Expression of these constructs was monitored in cell lysates as described in Fig. 6, and the capacity of anti-FLAG antibodies to immunoprecipitate (IP) the FLAG-tagged constructs was monitored, as was coimmunoprecipitation of the c-myc–tagged forms. N-TM3 + TM4 showed self-association, but N-TM5 + TM6 did not, whereas N-TM3 was unable to associate with N-TM3 + TM4.

of other aspects of class A GPCR function and the general understanding that homologous proteins have highly homologous structures.

Many of the studies to date, designed to identify GPCR interaction interfaces, have tested a limited number of possible interactions. However, given the observed organization of rhodopsin (Liang et al., 2003), we wished to examine potential sites of interaction generally and in an unbiased manner rather than testing one specific hypothesis. Previous studies using each of coimmunoprecipitation- (Carrillo et al., 2003; Stanasila et al., 2003; Uberti et al., 2003), FRET- (Carrillo et al., 2003, Stanisila et al., 2003), and functional reconstitution (Carrillo et al., 2003) -based approaches have provided evidence for dimerization of the α_{1b}-adrenoceptor. We have indicated previously a role of either TM1 or the N-terminal region of the α_{1b}-adrenoceptor because we could monitor a TR-FRET signal in intact cells between the full-length α_{1b}-adrenoceptor and a construct related to N-TM1 that was used to anchor a G protein α subunit in proximity to the receptor (Carrillo et al., 2003). We thus used combinations of coimmunoprecipitation and TR-FRET to measure interactions between different fragments of this receptor and their interactions with the full-length receptor to build a comprehensive interaction pattern map. The generated data are generally consistent with the cysteine cross-linking studies on the C5a receptor (Klco et al., 2003). Strong interactions were detected in each assay format indicative of symmetrical contact points involving both TM1 and TM4. Despite the clear contribution of TM1 to a symmetrical dimer interface, we were unable to disrupt this interaction by mutation of the glycophorin-A dimerization-like sequence present in TM1 of this receptor. These data are in agreement with those of Stanisila et al. (2003), who reached similar conclusions from less extensive mutational alteration of this site.

These results, however, are distinct from those of Overton et al. (2003), who showed that mutation of a similar sequence in the *S. cerevisiae* α factor receptor prevented the generation of a FRET signal. The current results clearly indicate that such glycophorin-A–like motifs do not generally serve this function in GPCRs. However, the genetic distance between yeast and mammalian systems and because these studies examined different GPCRs mean that it is not possible to

draw more general conclusions. Equally strong evidence supports a symmetrical TM4 interface in the quaternary structure of the α_{1b}-adrenoceptor. Again, this is consistent with cysteine cross-linking studies on the C5a receptor (Klco et al., 2003) and with related studies on the dopamine D2 receptor (Guo et al., 2003; Lee et al., 2003). However, a domain-swap study on the α_{1b}-adrenoceptor, in which one TM domain of the α_{1b}-adrenoceptor at a time was replaced with the equivalent section of the β_2-adrenoceptor, did not produce positive support for a contribution of TM4 (Stanisila et al., 2003). Furthermore, the TM domain-swap studies of Stanisila et al. (2003) indicated a role of TM7 in α_{1b}-adrenoceptor interactions. Apart from an early TM peptide-competition study on the dopamine D2 receptor (Ng et al., 1996), no other studies have implicated specific roles for TM7 in GPCR dimerization, and models (Klco et al., 2003) consistent with our data do not favor a key role of this region. We were unable to record any specific interactions of N-TM7 of the α_{1b}-adrenoceptor with either the full-length receptor or any other tested fragment of the receptor in these studies. Data consistent with symmetrical interactions involving both TM1 and TM4 might suggest two distinct means to generate an α_{1b}-adrenoceptor homodimer. Appropriate models can certainly be produced for both (Klco et al., 2003). However, although we cannot eliminate this possibility, a further possibility that is in keeping with the atomic-force microscopy studies on rhodopsin (Liang et al., 2003) is that the α_{1b}-adrenoceptor consists of higher-
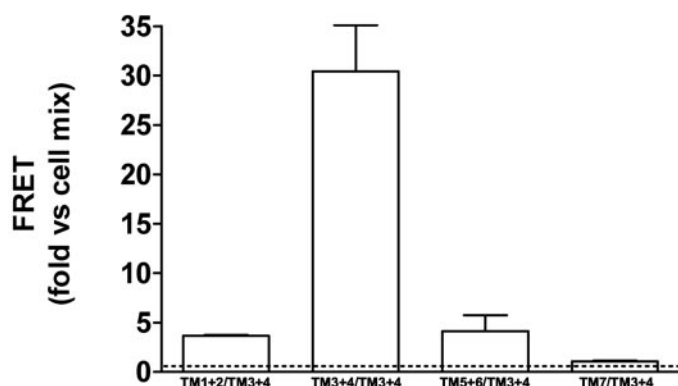
Fig. 12. Cell-surface self-association of TM3 + TM4. TR-FRET studies were performed in intact HEK293 cells after either coexpression of Flag N-TM3 + TM4 with c-myc N-TM1 + TM2, c-myc N-TM3 + TM4, c-myc N-TM5 + TM6, or c-myc N-TM7. Equivalent studies were performed in cells expressing each construct individually and mixed before analysis. Data are presented as the ratio of TR-FRET signal in coexpressing versus mixed cell populations.
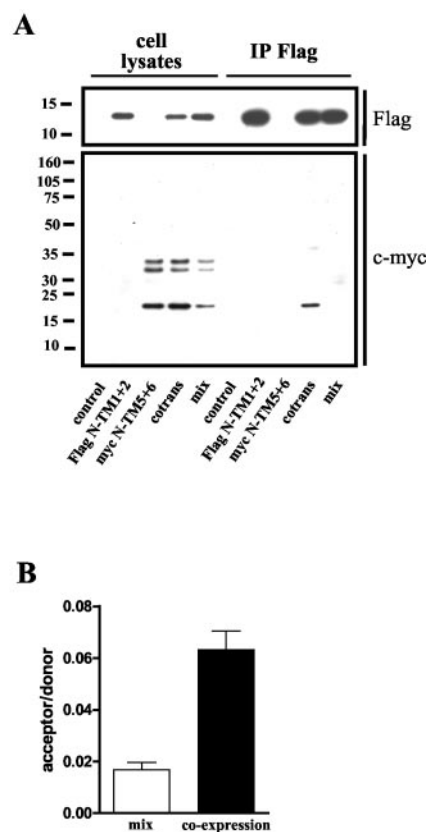
Fig. 13. Interactions between TM1 + TM2 and TM5 + TM6. Flag N-TM1 + TM2 and c-myc N-TM5 + TM6 were expressed individually or were coexpressed as in Fig. 8. A, appropriate expression patterns were confirmed by immunoblotting of cell lysates. Coimmunoprecipitation was achieved only from cells coexpressing the two fragments. B, TR-FRET monitored cell surface interactions. □, mixed cell population; ■, cells coexpressing the two constructs; IP, immunoprecipitation.

order oligomers or clusters. This would also be consistent with the observation of interactions of the N-TM5 + TM6 fragment with the full-length receptor and with N-TM1 + TM2 but with the lack of symmetrical interactions when differentially epitope-tagged forms of this fragment were coexpressed. Although caveats must be placed on the interpretation of coimmunoprecipitation studies involving full-length GPCRs (Salim et al., 2002), we note that in both these and many other studies, a substantial fraction of the precipitated receptor migrates with high apparent molecular mass. Although generally assumed to reflect nonspecifically aggregated proteins, it may, at least in part, also indicate a higher-order array or cluster of receptors. It is common to detect complexes with the characteristics of dimers or higher-order species that are resistant to SDS treatment in coimmunoprecipitation studies that use full-length GPCRs. However, with the exception of the symmetrical N-TM1–N-TM1 interaction, we observed little sign of the preservation of SDS-resistant polypeptide complexes when the coimmunoprecipitation studies used the α_{1b}-adrenoceptor fragments. This may also indicate the existence of and requirement for multiple interaction interfaces to strengthen the receptor oligomer. The evidence in favor of potential higher oligomer or cluster organization of the α_{1b}-adrenoceptor and the clear implication of symmetrical interactions involving both TM1 and TM4 raise the possibility of an interesting model. Given the orientation of the transmembrane helices in GPCR monomers and the available organizational density maps, symmetrical interactions between both TM1 and TM4 can be accommo-

dated in a chain of GPCRs (Fig. 14). It is interesting in this regard to note the "arrays" or strings of rhodopsin monomers noted in rod outer segments by Liang et al. (2003). Nonsymmetrical interactions observed between TM5, TM6, or the third intracellular loop with the TM1 + TM2 segment could then contribute to the organization of a molecular network of GPCRs.

Many of the studies herein used fragments of the receptor linked to a c-myc–tagged form of the N-terminal domain. Because the N-TM7 construct showed no detectable interactions with either the full-length receptor or the other receptor fragments, these studies provide no positive evidence for residues in the N-terminal section of the receptor being integral to the generation of receptor quaternary structure. As noted above, this is clearly very different from the situation with the class 3 GPCRs and from a small number of examples of class 1 GPCRs in which either the N-terminal sequence (Overton and Blumer, 2002) or glycosylation within this region (Xu et al., 2003) seems to contribute.

A number of studies have shown that the expression of certain fragments of GPCRs (Zhu and Wess, 1998; Lee et al., 2000) or even naturally occurring truncated variants (Coge et al., 1999; Karpa et al., 2000; Ding et al., 2002) are able to interact with full-length GPCRs and prevent effective cell-surface delivery. Herein, as monitored directly by fluorescence corresponding to APC-labeled anti-FLAG antibodies, coexpression of the various N-TM fragments did not significantly alter cell-surface delivery of the α_{1b}-adrenoceptor. It is interesting that although expressed, N-TM7 was not deliv-

TABLE 1

Interactions between fragments of the α_{1b}-adrenoceptor

Interactions (+) or lack of interactions (−) between N-terminally FLAG- and c-myc–tagged fragments of the α_{1b}-adrenoceptor were examined by either coimmunoprecipitation (square brackets) or TR-FRET (parentheses).

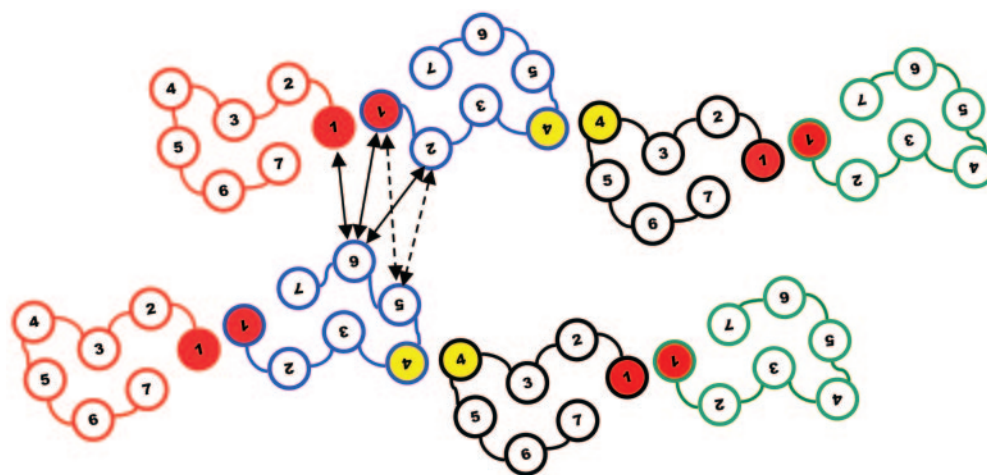|	c-myc N-TM1 + TM2	c-myc N-TM3 + TM4	c-myc N-TM5 + TM6	c-myc N-TM7
FLAG N-TM1 + TM2	[+] (N.D.)	[−] (N.D.)	[+] (N.D.)	[−] (N.D.)
FLAG N-TM3 + TM4	[−] (−)	[+] (+)	[−] (−)	[−] (−)
FLAG N-TM5 + TM6	[N.D.] (+)	[−] (−)	[−] (N.D.)	[−] (N.D.)

N.D., not determined.

Fig. 14. A macromolecular chain of α_{1b}-adrenoceptors can incorporate both symmetrical TM1-TM1 and TM4-TM4 interactions in a single model. Coimmunoprecipitation of α_{1b}-adrenoceptor fragments support symmetric interactions involving both TM1 and TM4. Although this may indicate two mechanisms to form distinct α_{1b}-adrenoceptor dimers, it is also consistent with the generation of a chain of α_{1b}-adrenoceptors that would seem similar to the "rows" of rhodopsin molecules observed by Liang et al. (2003). A model of such a row of α_{1b}-adrenoceptors and how this might interact with a second row of receptors is illustrated. Individual α_{1b}-adrenoceptor monomers are shown in different colors. Symmetric TM1-TM1 interfaces are noted in red and symmetric TM4-TM4 interactions in yellow. Possible nonsymmetric interactions consistent with those observed between the N-TM1 + TM2 and N-TM5 + TM6 fragments are labeled with arrows. These would allow a more complex network of α_{1b}-adrenoceptors to form.

MOL
PHARM

MOLECULAR PHARMACOLOGY

Downloaded from molpharm.aspetjournals.org by guest on December 1, 2012

ered effectively to the cell surface and equally was not coimmunoprecipitated when expressed with the full-length receptor. In contrast, when coexpressed with the full-length receptor, fragments such as N-TM1 + TM 2 and N-TM3 + TM4 were easily detected at the cell surface by direct monitoring of fluorescence derived from europium-labeled anti–c-myc antibodies. Although indirect, this could indicate that interaction with the full-length α_{1b}-adrenoceptor assisted in their cell-surface delivery. However, although no interactions were noted after coexpression of the N-TM1 + TM2 fragment of the α_{1b}-adrenoceptor with the full-length histamine H1 receptor, the N-TM1 + TM2 fragment was delivered to the cell surface. This was also the case when noninteracting fragments of the α_{1b}-adrenoceptor were coexpressed.

TR-FRET was used as a key approach in these studies to monitor the cell-surface expression of both full-length receptors and receptor fragments. The pattern of positive interactions of these fragments at the cell surface, monitored by TR-FRET, was entirely consistent with the immunoprecipitation studies (Table 1). It is difficult to interpret the magnitude of energy transfer signals because the physical basis of the signal is dependent on both the distance between energy donor and acceptor and their relative orientation (Milligan, 2004b). However, lack of energy transfer signal after coexpression of the N-TM1 + TM2 fragment of the α_{1b}-adrenoceptor with the human histamine H1 receptor is at least consistent with the positive signal obtained after coexpression of N-TM1 + TM2 with the full-length α_{1b}-adrenoceptor, reflecting a specific interaction. This complements previous data showing only weak interactions between the α_{1b}-adrenoceptor and the histamine H1 receptor obtained using completely distinct approaches (Carrillo et al., 2003).

These studies provide a comprehensive analysis of protein-protein interactions between TM-containing fragments of the α_{1b}-adrenoceptor that contribute to quaternary structure. The data are not compatible with the existence only of dimers resulting from a single symmetrical interaction between a specific TM domain. Although it is impossible to exclude the existence of only dimeric forms of the receptor that are generated by contacts between different sets of TM helices, these results are most consistent with the existence of clusters or arrays of the α_{1b}-adrenoceptor.

References

AbdAlla S, Zaki E, Lother H, and Quitterer U (1999) Involvement of the amino terminus of the B$_2$ receptor in agonist-induced receptor dimerization. *J Biol Chem* **274:**26079–26084.

Angers S, Salahpour A, Joly E, Hilairet S, Chelsky D, Dennis M, and Bouvier M (2000) Detection of β_2-adrenergic receptor dimerization in living cells using bioluminescence resonance energy transfer (BRET). *Proc Natl Acad Sci USA* **97:**3684–3689.

Armstrong D and Strange PG (2001) Dopamine D$_2$ receptor dimer formation: evidence from ligand binding. *J Biol Chem* **276:**22621–22629.

Ayoub MA, Couturier C, Lucas-Meunier E, Angers S, Fossier P, Bouvier M, and Jockers R (2002) Monitoring of ligand-independent dimerization and ligand-induced conformational changes of melatonin receptors in living cells by bioluminescence resonance energy transfer. *J Biol Chem* **277:**21522–21528.

Baneres JL and Parello J (2003) Structure-based analysis of GPCR function: evidence for a novel pentameric assembly between the dimeric leukotriene B4 receptor BLT1 and the G-protein. *J Mol Biol* **329:**815–829.

Canals M, Marcellino D, Fanelli F, Ciruela F, de Benedetti P, Goldberg SR, Fuxe K, Agnati LF, Woods AS, Ferre S, et al. (2003) Adenosine A$_{2A}$-dopamine D$_2$ receptor-receptor heteromerization: qualitative and quantitative assessment by fluorescence and bioluminescence energy transfer. *J Biol Chem* **278:**46741–46749.

Carrillo JJ, Pediani J, and Milligan G (2003) Dimers of class A G protein-coupled receptors function via agonist-mediated trans-activation of associated G proteins. *J Biol Chem* **278:**42578–42587.

Cheng ZJ and Miller LJ (2001) Agonist-dependent dissociation of oligomeric complexes of G protein-coupled cholecystokinin receptors demonstrated in living cells using bioluminescence resonance energy transfer. *J Biol Chem* **276:**48040–48047.

Coge F, Guenin SP, Renouard-Try A, Rique H, Ouvry C, Fabry N, Beauverger P, Nicolas JP, Galizzi JP, Boutin JA, et al. (1999) Truncated isoforms inhibit [^{3}H]prazosin binding and cellular trafficking of native human alpha1A-adrenoceptors. *Biochem J* **343:**231–239.

Cvejic S and Devi LA (1997) Dimerization of the δ opioid receptor: implication for a role in receptor internalization. *J Biol Chem* **273:**26959–26964.

Ding WQ, Cheng ZJ, McElhiney J, Kuntz SM, and Miller LJ (2002) Silencing of secretin receptor function by dimerization with a misspliced variant secretin receptor in ductal pancreatic adenocarcinoma. *Cancer Res* **62:**5223–5229.

Eidne KA, Kroeger KM, and Hanyaloglu AC (2002) Applications of novel resonance energy transfer techniques to study dynamic hormone receptor interactions in living cells. *Trends Endocrinol Metabol* **13:**415–421.

Filizola M and Weinstein H (2002) Structural models for dimerization of G-protein coupled receptors: the opioid receptor homodimers. *Biopolymers* **66:**317–325.

George SR, O'Dowd BF, and Lee SP (2002) G-protein-coupled receptor oligomerization and its potential for drug discovery. *Nat Rev Drug Discov* **1:**808–820.

Guo W, Shi L, and Javitch JA (2003) The fourth transmembrane segment forms the interface of the dopamine d2 receptor homodimer. *J Biol Chem* **278:**4385–4388.

Hebert TE, Moffett S, Morello J-P, Loisel TP, Bichet DG, Barret C, and Bouvier M (1996) A peptide derived from a β_2-adrenergic receptor transmembrane domain inhibits both receptor dimerization and activation. *J Biol Chem* **271:**16384–16392.

Jordan BA and Devi LA (1999) G-protein-coupled receptor heterodimerization modulates receptor function. *Nature (Lond)* **399:**697–700.

Karpa KD, Lin R, Kabbani N, and Levenson R (2000) The dopamine D3 receptor interacts with itself and the truncated D3 splice variant d3nf: D3–D3nf interaction causes mislocalization of D3 receptors. *Mol Pharmacol* **58:**677–683.

Klco JM, Lassere TB, and Baranski TJ (2003) C5a receptor oligomerization. I. Disulfide trapping reveals oligomers and potential contact surfaces in a G protein-coupled receptor. *J Biol Chem* **278:**35345–35353.

Kobilka BK, Kobilka TS, Daniel K, Regan JW, Caron MG, and Lefkowitz RJ (1988) Chimeric alpha 2-,beta 2-adrenergic receptors: delineation of domains involved in effector coupling and ligand binding specificity. *Science (Wash DC)* **240:**1310–1316.

Kunishima N, Shimada Y, Tsuji Y, Sato T, Yamamoto M, Kumasaka T, Nakanishi S, Jingami H, and Morikawa K (2000) Structural basis of glutamate recognition by a dimeric metabotropic glutamate receptor. *Nature (Lond)* **407:**971–977.

Lee C, Ji I, Ryu K, Song Y, Conn PM, and Ji TH (2002) Two defective heterozygous luteinizing hormone receptors can rescue hormone action. *J Biol Chem* **277:**15795–15800.

Lee SP, O'Dowd BF, Ng GY, Varghese G, Akil H, Mansour A, Nguyen T, and George SR (2000) Inhibition of cell surface expression by mutant receptors demonstrates that D$_2$ dopamine receptors exist as oligomers in the cell. *Mol Pharmacol* **58:**120–128.

Lee SP, O'Dowd BF, Rajaram RD, Nguyen T, and George SR (2003) D2 dopamine receptor homodimerization is mediated by multiple sites of interaction, including an intermolecular interaction involving transmembrane domain 4. *Biochemistry* **42:**11023–11031.

Liang Y, Fotiadis D, Filipek S, Saperstein DA, Palczewski K, and Engel A (2003) Organization of the G protein-coupled receptors rhodopsin and opsin in native membranes. *J Biol Chem* **278:**21655–21662.

Martin NP, Leavitt LM, Sommers CM, and Dumont ME (1999) Assembly of G protein-coupled receptors from fragments: identification of functional receptors with discontinuities in each of the loops connecting transmembrane segments. *Biochemistry* **38:**682–695.

McVey M, Ramsay D, Kellett E, Rees S, Wilson S, Pope AJ, and Milligan G (2001) Monitoring receptor oligomerization using time-resolved fluorescence resonance energy transfer and bioluminescence resonance energy transfer: the human δ opioid receptor displays constitutive oligomerization at the cell surface which is not regulated by receptor occupancy. *J Biol Chem* **276:**14092–14099.

Melnyk RA, Kim S, Curran R, Engelman DM, Bowie JU, and Deber CM (2004) The affinity of GxxxG motifs in transmembrane helix-helix interactions is modulated by long-range communication. *J Biol Chem* **279:**16591–16597.

Mercier JF, Salahpour A, Angers S, Breit A, and Bouvier M (2002) Quantitative assessment of beta 1- and beta 2-adrenergic receptor homo- and heterodimerization by bioluminescence resonance energy transfer. *J Biol Chem* **277:**44925–44931.

Milligan G (2004a) G protein-coupled receptor dimerization: function and ligand pharmacology. *Mol Pharmacol* **66:**1–7.

Milligan G (2004b) Applications of bioluminescence and fluorescence resonance energy transfer to drug discovery at G protein-coupled receptors. *Eur J Pharm Sci* **21:**397–405.

Milligan G, Ramsay D, Pascal G, and Carrillo JJ (2003) GPCR dimerisation. *Life Sci* **74:**181–188.

Ng GY, O'Dowd BF, Lee SP, Chung HT, Brann MR, Seeman P, and George SR (1996) Dopamine D2 receptor dimers and receptor-blocking peptides. *Biochem Biophys Res Commun* **227:**200–204.

Osuga Y, Hayashi M, Kudo M, Conti M, Kobilka B, and Hsueh AJW (1997) Co-expression of defective luteinizing hormone receptor fragments partially reconstitutes ligand-induced signal generation. *J Biol Chem* **272:**25006–25012.

Overton MC and Blumer KJ (2000) G-protein-coupled receptors function as oligomers in vivo. *Curr Biol* **10:**341–344.

Overton MC and Blumer KJ (2002) The extracellular N-terminal domain and transmembrane domains 1 and 2 mediate oligomerization of a yeast G protein-coupled receptor. *J Biol Chem* **277:**41463–41472.

Overton MC, Chinault SL, and Blumer KJ (2003) Oligomerization, biogenesis and signaling is promoted by a glycophorin A-like dimerization motif in transmembrane domain 1 of a yeast G protein-coupled receptor. *J Biol Chem* **278:**49369–49377.

Parmentier ML, Prezeau L, Bockaert J, and Pin JP (2002) A model for the functioning of family 3 GPCRs *Trends Pharmacol Sci* **23:**268–274.

Ramsay D, Carr IC, Pediani J, Lopez-Gimenez JF, Thurlow R, Fidock M, and Milligan G (2004) High affinity interactions between human α_{1A}-adrenoceptor C-terminal splice variants produce homo and hetero-dimers but do not generate the α_{1L}-adrenoceptor. *Mol Pharmacol* **66:**228–239.

Ramsay D, Kellett E, McVey M, Rees S, and Milligan G (2002) Homo- and hetero-oligomeric interactions between G-protein-coupled receptors in living cells monitored by two variants of bioluminescence resonance energy transfer (BRET): hetero-oligomers between receptor subtypes form more efficiently than between less closely related sequences. *Biochem J* **365:**429–440.

Rocheville M, Lange DC, Kumar U, Patel SC, Patel RC, and Patel YC (2000) Receptors for dopamine and somatostatin: formation of hetero-oligomers with enhanced functional activity. *Science (Wash DC)* **288:**154–157.

Salim K, Fenton T, Bacha J, Urien-Rodriguez H, Bonnert T, Skynner HA, Watts E, Kerby J, Heald A, Beer M, et al. (2002) Oligomerization of G-protein-coupled receptors shown by selective co-immunoprecipitation. *J Biol Chem* **277:**15482–15485.

Stanasila L, Perez J-B, Vogel H, and Cotecchia S (2003) Oligomerization of the α_{1a}- and α_{1b}-adrenergic receptor subtypes. *J Biol Chem* **278:**40239–40251.

Uberti MA, Hall RA, and Minneman KP (2003) Subtype-specific dimerization of α1-adrenoceptors: effects on receptor expression and pharmacological properties. *Mol Pharmacol* **64:**1379–1390.

White JH, Wise A, Main MJ, Green A, Fraser NJ, Disney GH, Barnes AA, Emson P, Foord SM, and Marshall FH (1998) Heterodimerization is required for the formation of a functional GABA$_B$ receptor. *Nature (Lond)* **396:**679–682.

Xu J, He J, Castleberry AM, Balasubramanian S, Lau AG, and Hall RA (2003) Heterodimerization of α2A- and β1-adrenergic receptors *J Biol Chem* **278:**10770–10777.

Zhu X and Wess J (1998) Truncated V2 vasopressin receptors as negative regulators of wild-type V2 receptor function. *Biochemistry* **37:**15773–15784.

Address correspondence to: Dr. Graeme Milligan, Molecular Pharmacology Group, Davidson Building, University of Glasgow, Glasgow G12 8QQ, Scotland, U.K. E-mail: g.milligan@bio.gla.ac.uk